Combust. Sci. and Tech., 1996, Vols. 116–117, pp. 479–498
Reprints available directly from the publisher
Photocopying permitted by license only

Formation and Destruction of Hexavalent Chromium in a Laboratory Swirl Flame Incinerator

WILLIAM P. LINAK[1,*] JEFFREY V. RYAN[1] and JOST O. L. WENDT[2]

[1]*Air Pollution Prevention and Control Division, National Risk Management Research Laboratory, U. S. Environmental Protection Agency, Research Triangle Park, NC USA 27711*
[2]*Department of Chemical and Environmental Engineering, University of Arizona, Tucson, AZ USA 85721*

(Received 26 June 1995; revised 7 November 1995)

The partitioning of chromium (Cr) in combustion systems was investigated theoretically and experimentally. Theoretical predictions were based on chemical equilibrium, and suggested that hexavalent chromium [Cr(VI)] was favored by the presence of chlorine (Cl), and diminished by the presence of sulfur (S). Experimental studies employed a 59 kW laboratory-scale combustor with a swirling natural gas diffusion flame through which aqueous Cr solutions were sprayed. Three types of experimental data were obtained. First, and most important, the overall Cr(VI) fraction of the total Cr in the exhaust was measured as a function of initial Cr valence [trivalent (III) or hexavalent], and Cl and S concentrations. Second, the size segregated distribution of Cr(VI) in the exhaust was explored for the Cr(III) waste feed with and without Cl and S. Third, the influence of waste feed Cr valence on the exhaust aerosol particle size distribution was determined. Analytical determinations of Cr(VI) and total Cr are described.

Results show that, for the high temperature, highly turbulent, gas-phase incinerator conditions examined, the relative ratio of Cr(VI)/total Cr is unaffected by the initial Cr valence of the waste, and ranged from near zero to approximately 8%, depending on the presence of S or Cl. Cl addition increased the fraction of Cr(VI) found in small particles (smaller than approximately 1.1 μm) from approximately 30 to 70%. In contrast to the chemical analysis, the particle size distribution (PSD) measurements indicate that the initial form of the Cr waste does influence the resultant PSD. This mechanism is not well understood, but a possible explanation is that at combustion temperatures the Cr speciation chemistry is equilibrium controlled, while the PSD is determined by the aerosol dynamics which are dependent on physical transformations and specific chemical pathways.

Keywords: Waste incineration; chromium speciation; hexavalent chromium; metal transformations

*corresponding author tel: (919) 541-5792 fax: (919) 541-0554 e-mail: blinak@inferno.rtpnc.epa.gov.

INTRODUCTION

Chromium (Cr) is a toxic metal with air emissions that are regulated in the U.S. by the Clean Air Act (CAA, 1990) and the Resource Conservation and Recovery Act (RCRA, 1986). RCRA, which regulates hazardous waste incinerators (HWIs) and boilers and industrial furnaces (BIFs) using hazardous waste fuels, currently uses risk assessment arguments to limit human exposure. Allowable ground level concentrations, to which the maximum exposed individual (MEI) is subjected, are determined based on Risk Specific Doses (RSDs) for four carcinogenic metals and Reference Air Concentrations (RACs) for eight non-carcinogenic metals (Federal Register, 1991; Garg, 1992). Only the hexavalent form of Cr [Cr(VI)] is considered to be a potent carcinogen, and its RSD is correspondingly very low (0.00083 $\mu g/m^3$). Data on Cr speciation in combustion exhaust gases are not readily available, and it is not clear that Cr(VI) is the dominant form, or even a significant portion, of total Cr in incinerator exhausts. However, for RCRA permitting purposes, all Cr is assumed to be Cr(VI) unless difficult site specific speciation is performed. Based on this assumption, Cr emissions are often a major contributor to the health risk assessments conducted at waste incineration facilities (Bailiff and Kelly, 1990).

Cr occurs in oxidation states ranging from divalent (II) to hexavalent (VI) (Goyer, 1991). However, only trivalent (III) and VI states are commonly found in the environment (Seigneur and Constantinou, 1995). Of these two, Cr(III) is the more abundant form with Cr(VI) compounds of greater industrial importance. Anthropogenic Cr in ambient air originates from fossil fuel combustion, waste incineration, and industrial sources such as ferrochrome processing, ore refining, and chemical, refractory, and cement production. Cr(III) oxide (Cr_2O_3) is present in high temperature refractories, and has been shown to promote sulfur (S) capture by calcium (Ca) products in hot combustion flue gases (Slaughter *et al.*, 1987). Anthropogenic sources account for 60–70% of the atmospheric Cr emissions, with natural sources accounting for the remaining 30–40% (Seigneur and Constantinou, 1995). Typical ambient concentrations of total Cr range from less than 0.0001 $\mu g/m^3$ in rural areas to 0.03 $\mu g/m^3$ in industrial cities (Goyer, 1991).

At ambient conditions, the vapor pressures of Cr species are negligible and only condensed phases are present. As a result, Cr atmospheric chemistry is associated with solid particles and aqueous droplets. Seigneur and Constantinou (1995) have reviewed the solution chemistry for Cr and developed a kinetic mechanism to describe the conversion of Cr(III) to Cr(VI) and Cr(VI) to Cr(III). They conclude that typical atmospheric conditions

favor the reduction of Cr(VI) to Cr(III) species through reactions with trivalent arsenic [As(III)], divalent iron [Fe(II)], vanadium (V), or sulfur dioxide (SO_2), although slow oxidation of Cr(III) to Cr(VI) is also possible under some extreme conditions through reactions with manganese (Mn).

There is no evidence that Cr(III) is converted to Cr(VI) in biological systems. However, Cr(VI), being a strong oxidizing agent, readily crosses cell membranes where it is reduced to Cr(III) (Trinchon and Feldman, 1989; Goyer, 1991). It has been speculated that the biological effects of Cr(VI) are associated with its biological mobility, reduction to Cr(III), and the formation of intracellular Cr(III) macromolecules (Goyer, 1991). With the exception of the lung, Cr does not bioaccumulate in the body (Trinchon and Feldman, 1989). Exposure to Cr(VI) is most commonly associated with cancer of the respiratory system, although other adverse health effects including skin ulcers, allergic dermatitis and nasal perforations have been identified (Trinchon and Feldman, 1989; Goyer, 1991).

In summary, Cr(VI), but not Cr(III), has been determined to pose a significant human health hazard. The ensuing health risk depends on exposure to Cr(VI), but not necessarily on exposure to total Cr. Since conversion of Cr(III) to Cr(VI) is unlikely through atmospheric or biological mechanisms (Seigneur and Constantinou, 1995; Goyer, 1991), the major route for human exposure is likely through direct (anthropogenic) releases of Cr(VI) into the environment. It is, therefore, important to determine what portion of total Cr emissions from combustion sources might consist of Cr(VI), and how this depends on combustion conditions, other fuel constituents, and the valence state of Cr entering the system.

The research reported here is concerned with both theoretical equilibrium predictions and experimental data. The experimental data were obtained from a laboratory-scale swirl diffusion flame test combustor operated at 59 kW. The intent was to conduct parametric experiments and to simulate practical conditions in a controlled manner, rather than to determine specific reaction rate constants and mechanisms. Significant effort was expended in improving sampling and analyses approaches for measuring Cr(VI) and total Cr. These efforts are described in detail. Results consist of partitioning Cr(VI) from non-Cr(VI) species, as a function of collected particle size.

THEORETICAL EQUILIBRIUM PREDICTIONS

Current models describing Cr partitioning in combustion systems are based on chemical equilibrium. These models have limitations, and it is important

to note that equilibrium may not be achieved in a particular system because of kinetic rate or mixing limitations. However, since only a very limited selection of gas-phase kinetic rate data involving Cr is available in the current literature (Smirnov, 1993; Fontijn *et al.*, 1994), detailed kinetic modeling of rates of formation of all important Cr species is not possible. Additionally, any equilibrium prediction is only as good as the thermochemical information available. Previous studies which included equilibrium predictions for Cr partitioning (Barton *et al.*, 1990; Linak and Wendt, 1993), had access to thermodynamic properties of only a limited number of Cr species. These studies predicted trends of increased volatility and increased Cr(VI) concentrations caused by large quantities of chlorine (Cl). In this study, equilibrium predictions were made using the CET89 computer code for calculating complex chemical equilibrium (Gordon and McBride, 1986).

Ebbinghaus (1993, 1995) has recently expanded the thermodynamic data base for Cr compounds both with and without Cl. Figure 1 shows equilibrium predictions using the Ebbinghaus thermochemistry, as well as the existing JANAF thermochemical data set (Chase, 1986) and data from Barin (1977, 1989). Cr(VI) species are represented by dashed lines. The Cr species considered are shown on Table I. The top panel (1a) shows Cr partitioning in the absence of Cl and S, and represents experimental methane (CH_4), oxygen (O_2), nitrogen (N_2), water (H_2O), and Cr input conditions shown on Table II. $CrO_2(OH)_2$(VI) is predicted to be stable in relatively low concentrations at intermediate and high temperatures (1200 and 2000 K). However, at temperatures less than 1700 K Cr speciation is dominated by Cr_2O_3 and CrO_2. The second panel (1b), shows Cr partitioning with 6,700 ppm Cl added to the incoming mixture (see Tab. II). A major change with respect to Cr(VI) partitioning occurs with the predicted formation of large quantities of vapor-phase $CrCl_6$(VI) at low temperatures (<700 K). Cl is thus expected to enhance the formation of Cr(VI). The third panel (1c) depicts the effect of S addition (7,900 ppm). Although some $CrO_2(OH)_2$ (VI) is predicted to be present at intermediate and high temperatures (1200 and 2000 K), the lower temperature (<800 K) region is completely dominated by trivalent $Cr_2(SO_4)_3$(III). The bottom panel (1d) shows that relatively small amounts of S (1100 ppm) with a large amount of Cl (6,700 ppm) are predicted to displace the chloride from the Cr salt and to form the $Cr_2(SO_4)_3$(III), replacing the $CrCl_6$(VI) (see Figs. 1b and 1d). Equilibrium predictions, therefore, suggest that: 1) although some Cr(VI) compounds are favored at high temperatures, they are not favored at low temperatures in the absence of Cl; 2) when Cl is added, Cr(VI) species are favored at stack

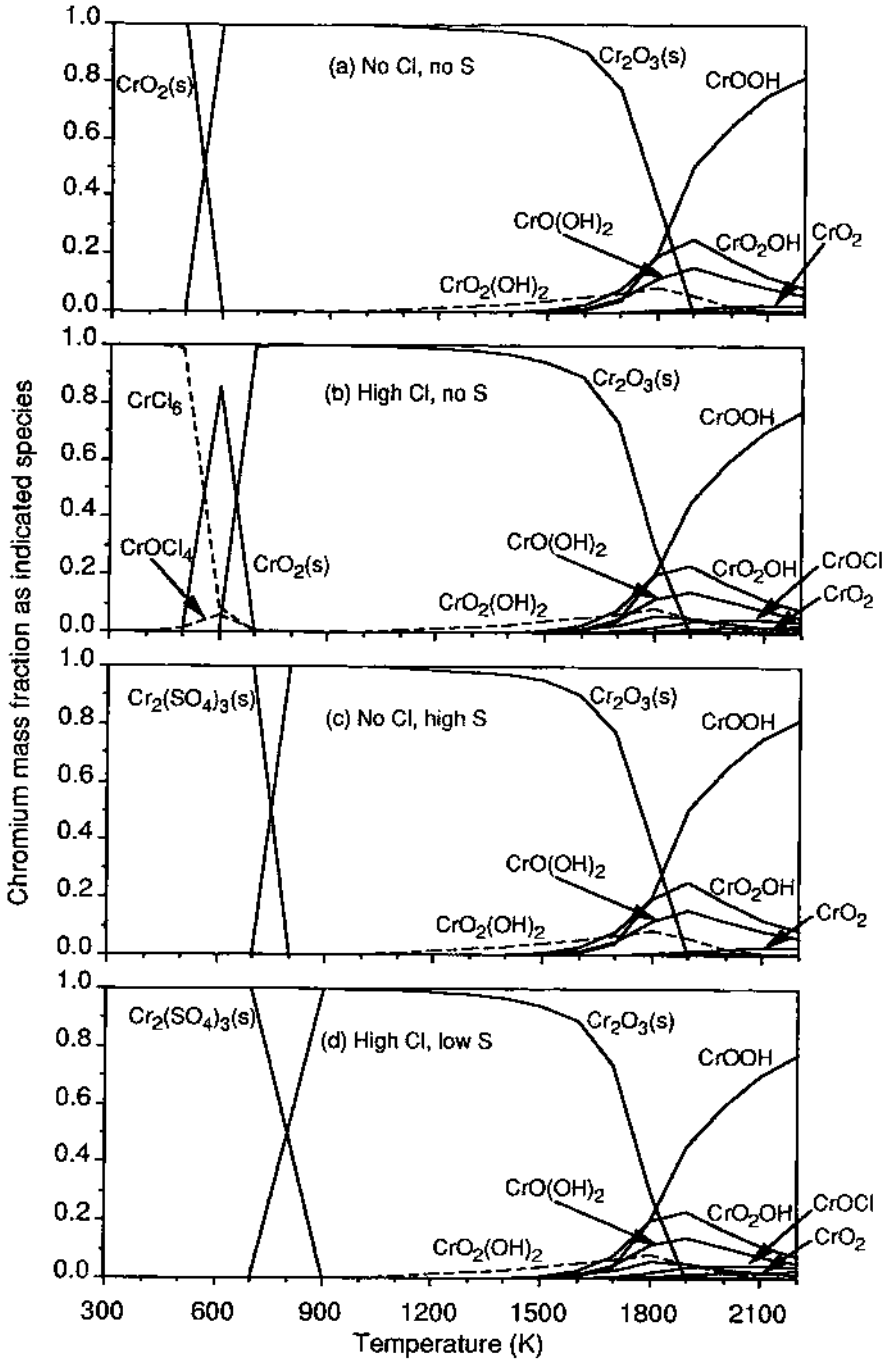

FIGURE 1 Chromium equilibrium predictions for four experimental conditions: (a) base case (no Cl, no S); (b) high Cl, no S; (c) no Cl, high S; and (d) high Cl, low S . Table 1 presents Cr species considered. Table 2 presents input concentrations used for calculations. Dashed lines represent Cr(VI) species.

TABLE 1 Chromium species considered during equilibrium analysis

Chromium species without chlorine or sulfur		*Additional species with chlorine*		*Additional species with sulfur*	
Species	*Reference*	*Species*	*Reference*	*Species*	*Reference*
Cr	J6/73	CrCl	BE95	CrS(1)	IB77
CrN	J12/73	$CrCl_2$	BE95	CrS(2)	IB77
CrO	J12/73	CrOCl	BE95	$Cr_2(SO_4)_3(s)$	IB89
CrOH	BE93	$CrCl_3$	BE95		
CrO_2	J12/73	$CrOCl_2$	BE95		
CrOOH	BE93	$CrCl_4$	BE95		
$Cr(OH)_2$	BE93	CrO_2Cl	BE95		
CrO_3	J12/73	$CrOCl_3$	BE95		
CrO_2OH	BE93	$CrCl_5$	BE95		
$Cr(OH)_3$	BE93	CrO_2Cl_2	BE95		
$CrO(OH)_2$	BE93	$CrOCl_4$	BE95		
$CrO_2(OH)_2$	BE93	$CrCl_6$	BE95		
$Cr(OH)_4$	BE93	$CrCl_2(s)$	IB89		
$CrO(OH)_4$	BE93	$CrCl_2(l)$	IB89		
$Cr(OH)_5$	BE93	$CrCl_3(s)$	IB89		
$Cr(OH)_6$	BE93				
$Cr(s)$	J6/73				
$Cr(l)$	J6/73				
$Cr_7C_3(s)$	IB89				
$Cr_{23}C_6(s)$	IB89				
$Cr(CO)_6(s)$	IB89				
$CrN(s)$	J12/73				
$Cr_2N(s)$	J12/73				
$CrO_2(s)$	IB89				
$CrO_3(s)$	IB89				
$CrO_3(l)$	IB89				
$Cr_2O_3(s)$	J12/73				
$Cr_2O_3(l)$	J12/73				

J6/73 : JANAF 6/73 - Chase (1986).
J12/73 : JANAF 12/73 - Chase (1986).
BE93 - Ebbinghaus (1993).
BE95 - Ebbinghaus (1995).
IB77 - Barin (1977).
IB89 - Barin (1989).

conditions; and 3) Cr(VI) disappears in the exhaust with the addition of relatively small amounts of S, even in the presence of larger amounts of Cl.

Experimental Apparatus and Experimental Procedure

Two types of data were desired. First, the speciation of Cr in the exhaust of a practical combustion system was investigated as functions of inlet Cr speciation (valence) and Cl and S content. Second, the influence of inlet Cr speciation on the exhaust aerosol particle size distribution (PSD) was deter-

TABLE II Experimental mass feed rates

Fuel/oxidant species	*feed rate*	*g-moles/min*	
CH_4	91.75 L/min	3.99	
O_2@ SR = 1.15	214.00 L/min	8.96	
N_2@ SR = 1.15	809.94 L/min	33.84	
Cr(III) tests	*feed rate*	*g-moles/min*	*Calculated stack ppm$_v$*
$Cr(NO_3)_3$(III)	1.25 g/min	0.00538	112 (Cr)
H_2O	17.50 g/min	0.969	
Cl_2 (low)	0.61 L/min	0.025	1040 (Cl)
SO_2 (low)	1.16 L/min	0.052	1090 (S)
Cl_2 (high)	3.79 L/min	0.159	6700 (Cl)
SO_2 (high)	7.45 L/min	0.379	7900 (S)
Cr(VI) tests	*feed rate*	*g-moles/min*	*Calculated stack ppm$_v$*
CrO_3(VI)	0.52 g/min	0.00518	108 (Cr)
H_2O	17.50 g/min	0.969	
Cl_2 (low)	0.61 L/min	0.025	1040 (Cl)
SO_2 (low)	1.16 L/min	0.052	1090 (S)
Cl_2 (high)	3.79 L/min	0.159	6700 (Cl)
SO_2 (high)	5.04 L/min	0.256	5400 (S)

mined. Both speciation and particle size affect the health risks associated with Cr aerosol air emissions.

Laboratory Swirl Flame Incinerator

Experiments were performed using the laboratory-scale 59 kW (actual), 82 kW (maximum rated) horizontal tunnel combustor presented in Figure 2. This refractory-lined research combustor was designed to simulate the time/temperature and mixing characteristics of practical industrial liquid and gas waste incineration systems. Fuel, surrogate wastes, and combustion air were introduced into the burner section through an International Flame Research Foundation (IFRF) moveable-block variable air swirl burner. This burner incorporates an interchangeable injector positioned along its center axis. Swirling air passes through the annulus around the fuel injector promoting flame stability and attachment to the water-cooled quarl. For the research results presented here a high swirl (IFRF type 2) flame with internal recirculation (Swirl No. = 1.48) was used. Axial access ports permitted temperature measurement (Linak *et al.*, 1994). Gaseous and aerosol samples were taken from a stack location 589.3 cm from the burner quarl.

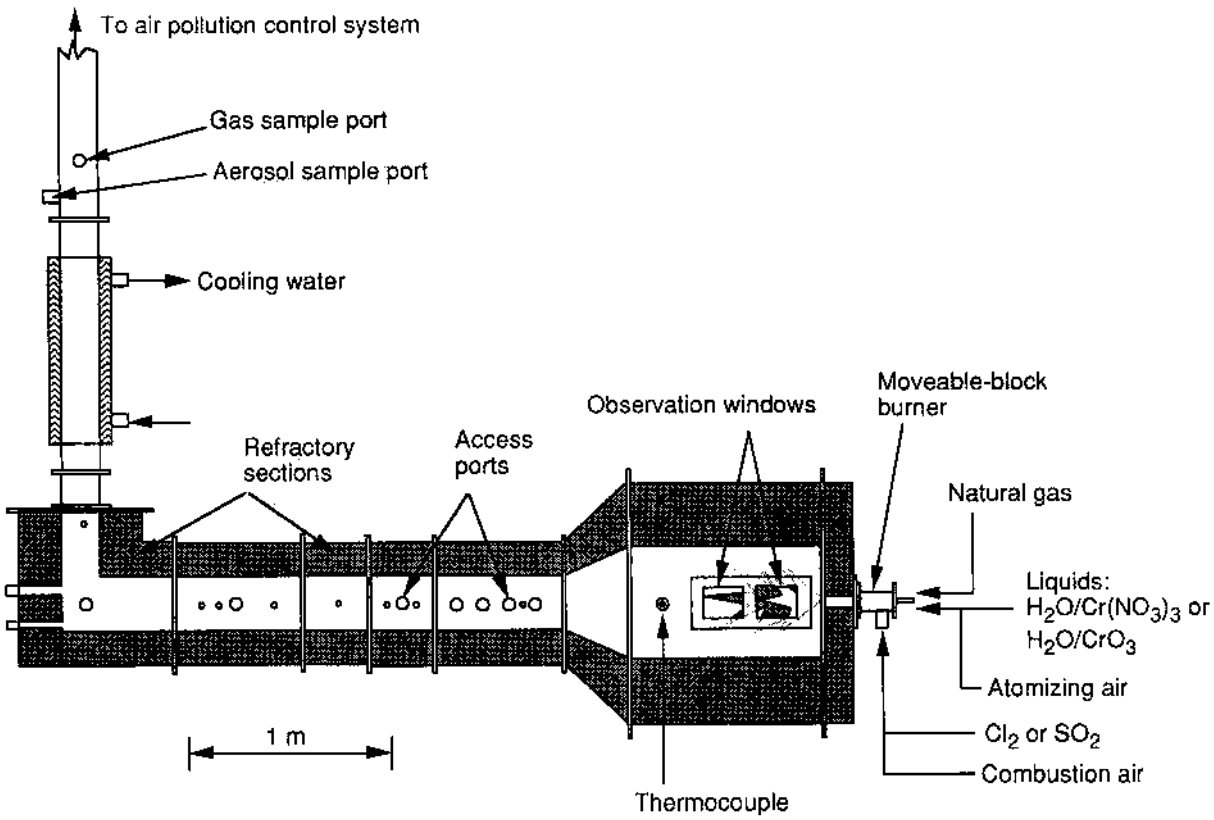

FIGURE 2 EPA horizontal tunnel combustor.

The temperature at this location was approximately 670 K (745°F). Further details regarding the experimental combustor can be found elsewhere (Linak *et al.*, 1994, 1995).

Cr(III) nitrate [$Cr(NO_3)_3$] or Cr(VI) oxide (CrO_3) was introduced as aqueous solutions through a special fuel waste injector which incorporated a small air atomizing system down the center of a standard natural gas injector. The resulting droplet PSD was relatively narrow with a mean droplet diameter of approximately 50–80 μm (Linak *et al.*, 1994). Diatomic chlorine (Cl_2) or SO_2 were introduced, separately from the metal solutions, with the (secondary) combustion air. Thus, the metal, Cl or S, was not mixed prior to its introduction into the combustor. All interactions between the components were dependent upon normal mixing patterns.

Chromium Systems Investigated

Experiments were performed injecting aqueous solutions of $Cr(NO_3)_3$(III) and CrO_3(VI) with and without Cl_2 or SO_2, into a 59 kW (200,000 Btu/hr) natural gas flame. Aqueous solutions containing 1.5% (by weight) Cr were used. Solution flow rates were maintained so as to produce stack gas concentrations of approximately 100 ppm Cr (by volume). $Cr(NO_3)_3$(III) and CrO_3(VI) feed rates were 1.25 and 0.52 g/min., respectively, and correspond to constant molar feed rates of 0.005 g-moles/min. The tests were designed to introduce Cl_2 or SO_2 to maintain either a 10:1 or 100:1 molar ratio of Cl or S to metal, resulting in intended Cl or S stack concentrations of approximately 1000 and 10,000 ppm (by volume). These correspond to low Cl, low S and high Cl, high S conditions, respectively. In practice, however, while the 1000 ppm low Cl and low S conditions were achieved (approximately), gas flows limited the high Cl tests to approximately 6700 ppm and the high S tests to between 5400 and 7900 ppm. Excess air was maintained at 15%. No air preheat was employed. Cl_2 or SO_2 gases were introduced with the combustion air. Experimental mass feed rates are presented in Table II.

Chromium Speciation: Sampling and Analysis

Measurement of Cr partitioning is difficult for two reasons: First, the dominant Cr species predicted by equilibrium [Cr_2O_3(s), see Fig. 1] is a condensed species which is difficult to digest for subsequent analysis. Second, care must be taken to ensure that Cr(VI) is not reduced during the sampling and analysis process. This is usually accomplished by keeping the sample in

contact with an alkaline environment at all times. The converse problem of Cr oxidation to Cr(VI) species is not an issue at room temperatures (Seigneur and Constantinou, 1995).

Two sets of experiments were performed to determine factors which influenced the partitioning of Cr in the exhaust. The first set of experiments used $Cr(NO_3)_3$(III) as the metal waste, and investigated size segregated speciation of the exhaust aerosol. This set uncovered problems related to total Cr analysis, although the Cr(VI) analyses were sound. The first set, therefore, provides data on what fraction of the Cr(VI) consists of vapor-phase species and submicron particles, compared to supermicron particles [with $Cr(NO_3)_3$(III) as the waste feed], although it was unable to determine the Cr(VI)/total Cr partitioning which was the principal objective of these experiments. The second set of experiments were conducted after the total Cr analytical problem was solved and therefore, did address Cr(VI)/total Cr partitioning for both $Cr(NO_3)_3$ and CrO_3 waste feeds. Data from this set comprise all the speciation data presented. Size segregated speciation data, however, were not obtained from this data set, since an EPA draft Method 0013 (1990) sampling protocol was used rather than a dilution probe and cascade impactor system (Linak *et al.*, 1994). Draft Method 0013 does not provide for particle size classification.

The first set of five experiments (concentrations shown in Tab. II) included baseline (no Cl, no S), low Cl, high Cl, low S, and high S conditions with $Cr(NO_3)_3$(III) as the waste feed. The exhaust aerosol was sampled with a dilution probe (Linak *et al.*, 1994), and size segregated into two fractions using a modified Andersen cascade impactor. Particles greater than approximately 1.1 μm diameter were collected on 81 mm quartz fiber filter substrates on three impactor stages, and subsequently frozen to prevent the reduction of collected Cr(VI). Vapor-phase species and particles less than approximately 1.1 μm diameter passed through the impactor and were directed to two impingers, each containing 100 mL of a 0.5 N potassium hydroxide (KOH) solution, following the stabilizing approach of EPA Draft Method 0013 (1990). Samples were collected at a nominal flow rate of 1 scfm (28.3 sL/min.). Nominal test duration was 45 min. Following sample collection, the impinger contents were weighed, the alkaline pH verified, and the contents transferred to clean, amber glass sample jars. The impingers and connecting glassware were rinsed with deionized water and the rinsates combined with the impinger sample. The impingers and connecting glassware were then rinsed again with 0.1 N nitric acid (HNO_3), and this rinsate was collected in separate sample jars. The sample jars were kept refrigerated until submitted for analysis.

The samples were analyzed for both Cr(VI) and total Cr. Cr(VI) analyses were performed using ion chromatography with a post-column reactor (IC/PCR) and a visible wavelength detector as described in the Method Manual for Compliance with BIF Regulations (Draft Method 0013, 1990). The three particle filters (impactor stages) were combined and leached with 50 mL of 0.1N KOH for 2 hours. The extract was brought to a volume of 50 mL. Except for the determination of total sample volumes, no further preparation of the impinger samples was required. An aliquot of each caustic impinger solution and caustic filter (impactor) extract was then analyzed [for Cr(VI)] by IC/PCR.

These same sample fractions were also analyzed for total Cr by graphite furnace atomic absorption (GFAA) spectrometry. Prior to analysis, aliquots of the samples were acid digested using concentrated HNO_3. This procedure is intended both to reduce the Cr(VI) species and to solubilize other Cr species. Each aliquot was concentrated to near dryness using a hot plate. Next, 10 mL of concentrated HNO_3 was added, and the samples were further concentrated to approximately 5 mL. The acid impinger rinsates were also acid digested and analyzed separately. The concentrates were then filtered, brought to a volume of 50 mL, and analyzed by GFAA.

However, these tests failed to yield satisfactory total Cr mass balance closure. Comparison of measured Cr emissions to theoretical emissions demonstrated unacceptable recoveries, typically less than 1%. Possible problem areas included poor Cr atomization through the burner, loss of Cr to refractory and combustor surfaces, sampling errors, and unknown analytical interferences, including incomplete sample digestion. The last-mentioned was a prime suspect for the major portion of the discrepancy, since green filtrates were observed after supposed digestion with concentrated HNO_3.

Sample digestion was further investigated, using a sample of analytical grade Cr_2O_3(III). The appearance of this material was virtually identical to that of the HNO_3 filtrates. Two alternative digestion procedures were evaluated prior to the analysis of the second set of flue gas samples. The first method evaluated the hydrofluoric acid (HF) digestion procedure used to digest filter samples collected by draft Method 29 (1990). The second method was a caustic fusion technique.

For the HF digestion procedure, 150 mg of analytical grade Cr_2O_3(III) (which is approximately equal to the mass of total Cr calculated to be present in the stack gas samples), 6 mL of concentrated HNO_3, and 4 mL of concentrated HF were placed in a microwave pressure relief vessel. Each sample was heated for 15 min. in 2 min. intervals at 600 W, diluted to 100

mL in a volumetric flask, and analyzed by GFAA as described above. Digestion efficiencies of 44 and 72% were observed for the duplicate samples, respectively.

For the caustic fusion procedure, approximately 50 mg of Cr_2O_3(III) was placed in a graphite crucible and "fused" with 1 g of sodium nitrate ($NaNO_3$) and 3 g of sodium hydroxide (NaOH) in a muffle furnace. During fusion, the crucible and contents were heated over a 4 hour period from 250 to 410 °C with 1 hour stops at 350 and 390 °C. Upon cooling, the sample was dissolved in approximately 60 mL of deionized water over a hot plate and then diluted to 100 mL in a volumetric flask with 2 mL of concentrated HNO_3 added. The digested samples were analyzed by GFAA as described above. Digestion efficiencies of 75, 87, and 91% were observed for the triplicate samples, respectively. Based on these measured digestion efficiencies, the caustic fusion technique was selected for determining total Cr.

The second set of combustion experiments, which focused on Cr speciation, strictly followed guidelines outlined in draft Method 0013 (1990), an established and verified sampling and analytical procedure for Cr(VI). Unfortunately, draft Method 0013 includes a caustic solution quench within a quartz sampling probe and, thus, does not allow for size segregation of the collected sample. However, it should be noted that, once Cr(VI) was determined using the draft Method 0013 analytical procedure, the samples were redigested using the caustic fusion procedure and analyzed for total Cr. This involved concentrating the caustic solutions to near dryness on a hot plate and then following the caustic fusion procedure outlined above.

While analytical recoveries using the caustic fusion method were high, typical Cr recovery mass balances through the combustor ranged from 25 to 30%. It was noted that the Cr feed streams were difficult to atomize and often formed growing appendages on the injection nozzle, and this would account for significant mass loss. In addition there may have been losses to the refractory walls.

Aerosol Particle Size Distribution: Sampling and Analysis

PSD measurements were taken from the stack using an Andersen eight stage, 28.3 L/min. (1 ft^3/min.), atmospheric pressure cascade impactor and a TSI differential mobility particle sizer (DMPS) (Linak *et al.*, 1994). The cascade impactor is designed to collect physical samples (for subsequent gravimetric and/or chemical analysis) on nine stages (including the after-filter) less than approximately 10 μm diameter. The DMPS classifies and

counts particles within a working range of 0.01 to 1.0 μm diameter using principles of electrical mobility. The DMPS was configured to yield 27 channels evenly spaced (logarithmically) over this range.

Cascade impactor and DMPS samples were taken using a two-stage isokinetic aerosol sampling system based on the modified designs of Scotto *et al.* (1992). Detailed discussion of its operation is presented elsewhere (Linak *et al.*, 1994). In order to minimize in-probe gas and aerosol kinetics, the sampling system dilutes and cools the aerosol sample using filtered N_2 and air immediately after sampling. Calculated dilution ratios and sampling probe residence times are approximately 20:1 and 0.2 s, and 400:1 and 2.5 s for the impactor and DMPS, respectively. Dilution ratios are measured directly for each experiment and verified independently by the measurement of a nitric oxide tracer gas.

Results and Discussion

Three types of data are presented. First, the overall Cr(VI) fraction of the total Cr in the exhaust, was measured as a function of initial Cr valence [Cr(III) or Cr(VI)], and Cl and S concentration. These data resulted from use of the draft Method 0013 sampling and analytical protocol for Cr(VI), and subsequent redigestion of the samples using the caustic fusion method. Second, the size segregated distribution of Cr(VI) in the exhaust was explored for the Cr(III) waste feed, with and without Cl and S. Third, DMPS and impactor measurements investigated how Cr speciation [$Cr(NO_3)_3$(III) or CrO_3(VI)] in the feed, influences the exhaust aerosol PSD. Results are interpreted as they are presented.

Cr(VI)/Total Cr Partitioning

The bar graphs on Figure 3 depict the overall partitioning between Cr(VI) and total Cr. In the upper panel (3a), Cr partitioning results from the introduction of $Cr(NO_3)_3$(III) in aqueous solution are presented. With neither Cl nor S present, approximately 2% of the total Cr in the stack gas effluent is hexavalent. Addition of 1000 ppm (low) Cl increased the percent Cr(VI) in the exhaust slightly to 2.5%. Addition of 6,700 ppm (high) Cl raised the Cr(VI) percentage in the exhaust to approximately 8%. The addition of S (no Cl present) sharply diminished the emission of Cr(VI). In fact, with a high concentration of S (7,900 ppm), the Cr(VI) percentage was

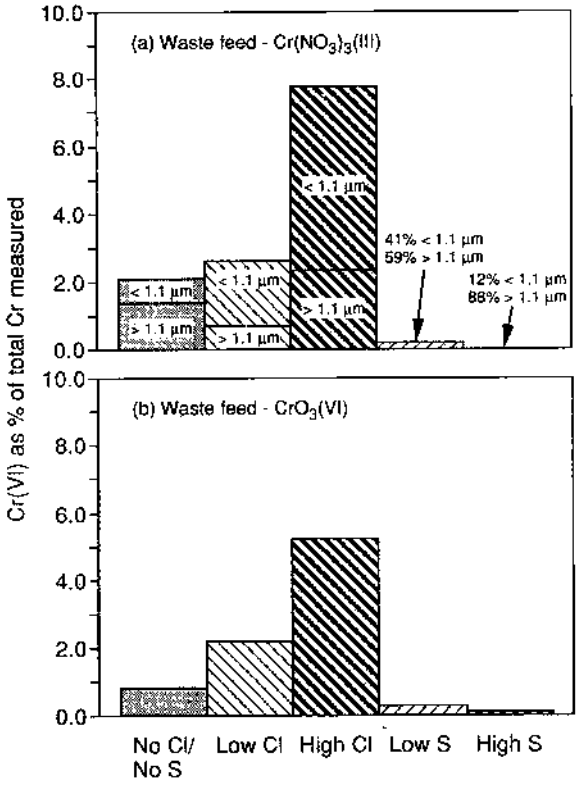

FIGURE 3 Cr(VI) mass as a percent of total Cr mass measured in the stack gases as a function of Cr waste feed valence and acid gas added: (a) $Cr(NO_3)_3$(III) waste feed; (b)CrO_3(VI) waste feed. The upper panel (a) denotes the mass fraction of Cr(VI) found in particles greater or less than 1.1 µm diameter.

reduced to near detection levels. The differences in Cr(VI)/total Cr shown on Figure 3 are due primarily to large differences in the absolute amounts of Cr(VI) measured, rather than to differences in total Cr measured. Thus, it is unlikely that these results are corrupted by sample digestion difficulties.

The trends exhibited in Figure 3a, are consistent with equilibrium predictions, although the absolute values are not. In the absence of both Cl and S, some Cr(VI) which is stable at higher temperatures appears to persist through to the lower temperature regime, even though equilibrium would not predict its presence there. High Cl concentrations sharply enhanced Cr(VI) emissions, possibly due to $CrCl_6$ which was predicted to be stable at low temperatures. The effect of S is consistent with equilibrium if it is assumed that conversion of Cr to $Cr_2(SO_4)_3$ is rapid. It is interesting that

equilibrium predicts that even relatively small quantities of S can counteract the Cr(VI) formation tendencies of Cl.

In the lower panel (3b), analogous results are presented for CrO_3(VI) waste feed. It is significant that they are very similar to the results presented in the top panel (3a) with Cr(III) waste feed. The partitioning of Cr in a combustor thus seems to be independent of the initial valence of Cr waste feed. Most of the Cr(VI) that entered was converted to Cr(III). The similarity in partitioning between the upper and lower panels of Figure 3, and the fact that the final Cr(VI)/total Cr partitioning is independent of initial speciation, suggests that prior to sampling, some type of equilibrium controlled mechanism, with neither kinetic nor mixing limitations, is operable. However, the low conversion to Cr(VI) in the presence of Cl, and the finite conversion in the absence of Cl and S, suggest that this equilibrium is "frozen" at a temperature higher than the sampling or exhaust temperature.

Size Segregated Cr(VI) Distribution

Also shown on Figure 3a is the fraction of the Cr(VI) found on particles larger than approximately 1.1μm meter, and the fraction found as vapor or on particles less than that size. Of interest was how the size segregation of Cr(VI) varied with presence of Cl and S, for a given Cr waste [in this case, $Cr(NO_3)_3$]. These fractions were actually obtained from experiments where total Cr was not measured and were assumed to be valid when applied to the other experiments where total Cr was determined (for the same waste and acid gas conditions). They could thus be included on Figure 3a, as shown. Cr(VI) mass greater than 1.1 μm diameter was analyzed from particles found on impactor filter substrates. Cr(VI) mass less than 1.1 μm diameter passed through the impactor into the caustic impinger solutions. For the base case, with no acid gas, most of the Cr(VI) was associated with the larger particles. With Cl, a larger fraction (approximately 70%) was found in the submicron particle size range. The latter result is consistent with the high volatility of $CrCl_6$, and has implications from a health effects perspective.

Particle Size Distributions

Figure 4 shows DMPS and impactor PSDs for the exhaust aerosol for the $Cr(NO_3)_3$(III) and CrO_3(VI) waste feeds. There is no added Cl or S. For $Cr(NO_3)_3$ (open circles), the base case PSDs indicate relatively low volume

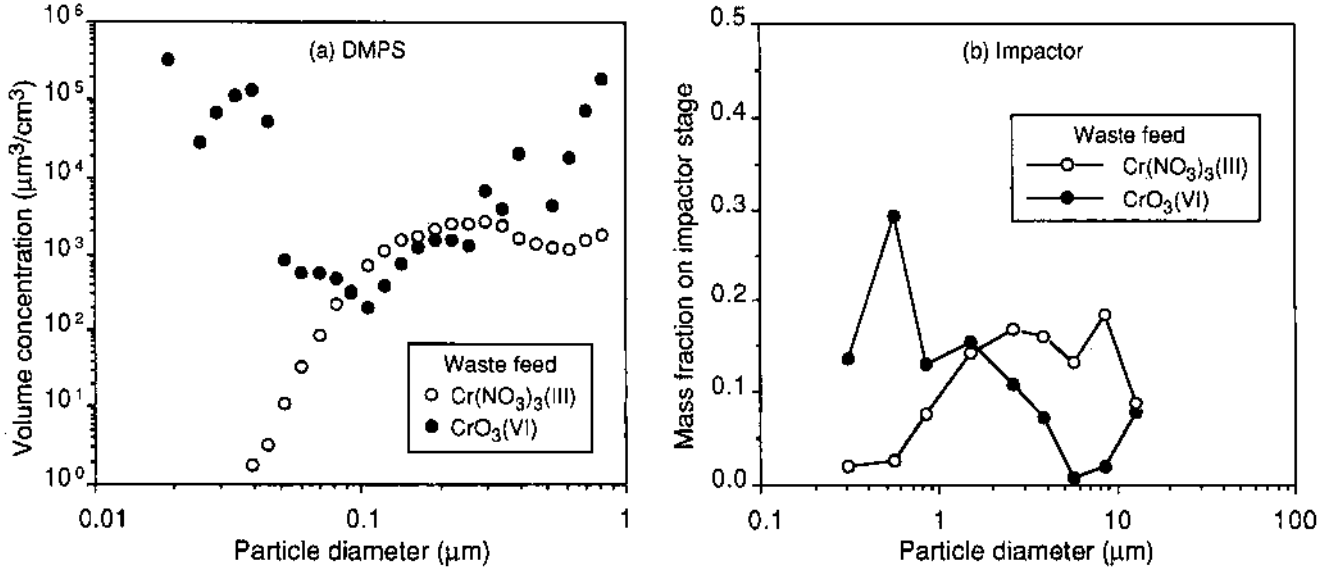

FIGURE 4 (a) DMPS submicron volume distribution and (b) impactor mass fraction distribution for $Cr(NO_3)_3$(III) and CrO_3(VI) waste feeds.

concentration of submicron particles (approximately 10^3 $\mu m^3/cm^3$), with the majority of the aerosol mass evenly distributed in particle sizes between 2 and 10 μm diameter. When CrO_3(VI) is used as the waste feed (shaded circles), the submicron volume concentrations (DMPS) are notably higher than those for the $Cr(NO_3)_3$(III) waste feed (10^5 vs 10^3 $\mu m^3/cm^3$). Also, well defined submicron nuclei modes (0.04–0.05 μm) are seen for CrO_3 waste feed case only. These DMPS data are also consistent with the impactor data. These results, combined with the Cr(VI) partitioning data presented in Figure 3, suggest that mechanisms which control Cr(VI) partitioning and Cr PSDs are different. Chemical analyses (Fig. 3) suggest that the original valence of the Cr waste does not influence the resultant Cr(VI)/total Cr partitioning and that this behavior is consistent with thermodynamic predictions (Fig. 1). However, the PSD data indicate that the original Cr speciation strongly influences the resultant PSD. Based on the PSDs, and the assumption that the atomization characteristics of the two solutions are not significantly different to account for a factor of 10 or more change in the atomized liquid drop sizes, $Cr(NO_3)_3$(III) solutions appear to form approximately one residual particle per droplet, whereas, the CrO_3(VI) solutions form multiple particles per droplet.

Therefore, it seems likely that the CrO_3(VI) either volatilizes itself or passes through a volatile intermediate while the $Cr(NO_3)_3$(III) does not, although the ultimate speciation [predominantly Cr_2O_3(III)] is the same for both. Scanning electron micrographs showed no evidence of fractured cenospheres for either $Cr(NO_3)_3$(III) or CrO_3(VI), thus eliminating fragmentation as an important mechanism.

CONCLUSIONS

For the high temperature, highly turbulent, gas-phase incinerator conditions examined here, the relative ratio of Cr(VI)/total Cr is unaffected by the initial Cr valence of the waste, and ranges from near zero to approximately 8%, depending on the presence of Cl or S. Comparison of the equilibrium predictions and Cr(VI)/total Cr partitioning data suggests that under flame conditions, Cr speciation is determined by high temperature equilibrium, with neither kinetic nor mixing limitations to prevent that high temperature equilibrium from being attained. Equilibrium predictions indicate that, although some Cr(VI) species are stable at high temperatures, they are not favored at low temperatures in the absence of Cl. Data, however, show that, without available Cl, 2% (or less) of the total Cr exists as Cr(VI). When Cl

is added, equilibrium predicts Cr(VI) species to be favored at stack conditions, while the data indicate that Cr(VI) species increase, but only to between 5 and 8% of the total Cr measured. The equilibrium prediction and data also indicate that the presence of S greatly inhibits the formation of Cr(VI) species. With S addition, the data show that less than 0.5% of the total Cr is partitioned to Cr(VI) species. Although not examined experimentally, it is interesting to note that equilibrium also predicts relatively small amounts of S to inhibit the formation of Cr(VI) species even in the presence of large amounts of Cl. However, the low conversion to Cr(VI) in the presence of Cl, and the finite conversion in the absence of Cl and S, suggests that this equilibrium is "frozen" at a temperature higher than the sampling or exhaust temperature and the process then becomes kinetically controlled. In contrast to the chemical analysis, PSD measurements indicate that the initial form of the Cr waste does influence the resultant PSD. This mechanism is not well understood. A possible explanation is that although the Cr speciation chemistry may be equilibrium controlled at some high temperature, the PSD is determined by the aerosol dynamics which are dependent on physical transformations and specific chemical pathways.

In summary, the results suggest that Cr(VI) species may actually be only a small fraction of the total Cr emitted in the stack gases from incineration/combustion systems, and that this fraction is dependent on acid gas concentrations, but not on the initial waste Cr valence. It should be noted, in this regard, that Cr species, and in particular Cr_2O_3, can be very difficult to digest in the standard acids used for total Cr determination. The caustic fusion technique improved Cr digestion efficiencies over those measured using the HF digestion procedure outlined in draft Method 29. The results also suggest that, even in the presence of Cl, Cr(VI) emissions may be minimized by the addition of small amounts of S which presumably promote the formation of $Cr_2(SO_4)_3$(III). This process modification may offer a control procedure to ensure minimal emissions of Cr(VI) from incineration/combustion systems.

Acknowlegments/Disclaimer

Portions of this work were conducted under EPA P.O. 4D2910NATX with J.O.L. Wendt and EPA Contract 68-D4-0005 with Acurex Environmental Corp. The authors would like to gratefully acknowledge the valuable contributions of S. Davis, T. Lombardo, C. Elmore, R. Thomas, and D. Janek of Acurex Environmental Corp. to the modeling and experimental efforts as

Goyer, R. A. (1991). Toxic effects of metals, in Casarett and Doull's toxicology the basic science of poisons, 4th ed., Amdur, M.O., Doul, J. and Klaassen, C.D., eds., Pergamon Press, New York, NY.

Linak, W. P. and Wendt, J. O. L. (1993). Toxic metal emissions from incineration: mechanisms and control, *Prog. Energy Combust. Sci.*, **19**, 145–185.

Linak, W. P., Srivastava, R. K. and Wendt, J. O. L. (1995). Sorbent capture of nickel, lead, and cadmium in a laboratory swirl flame incinerator, *Combust. & Flame*, **100**, 241–248.

Linak, W. P., Srivastava, R. K. and Wendt, J. O. L. (1994). Metal aerosol formation in a laboratory swirl flame incinerator, *Combust. Sci. and Technol.*, **101**(1–6), 7–27.

RCRA - Resource Conservation and Recovery Act, Subtitle C, Sections 3001–3013, 42 N.S.C., Sections 6921–6934 (1976) and Supplement IV (1980) amended (1986).

Scotto, M. A., Peterson, T. W. and Wendt, J. O. L. (1992). Hazardous waste incineration: the in-situ capture of lead by sorbents in a laboratory down-flow combustor, *24th Comb. (Int.) Symp.*, 1109–1118, *Comb. Inst.*, Pittsburgh.

Seigneur, C. and Constantinou, E. (1995). Chemical kinetic mechanism for atmospheric chromium, *Environ. Sci. and Technol.*, **29**, 222–231.

Slaughter, D. M., Thomson, W. J., Peterson, T. W., Chen, S. L., Seeker, W. R. and Pershing, D. W. (1987). Influence of coal mineral matter on the effectiveness of dry sorbent injection for SO_2 control, EPA-600/7–87–020 (NTIS PB88-178587), Research Triangle Park, NC.

Smirnov, V. N. (1993). On the anomalously high rate of recombination $Cr + O_2 + M \rightarrow CrO_2 + M$, *Kinetics and Catalysis*, **34(5)**, 699–703.

Trinchon, M. and Feldman, J. Chemical kinetic considerations of trace toxic metals in incinerators, Incineration Conference, Knoxville, TN, May 1989.

well as the contribution of K. Luk of Research Triangle Institute, for the caustic fusion digestion procedure. The authors would also like to thank W.R. Seeker and R.G. Rizeq, of Energy and Environmental Research Corp. for providing much of the thermodynamic data. The research described in this article has been reviewed by the Air Pollution Prevention and Control Division, U.S. Environmental Protection Agency, and approved for publication. The contents of this article should not be construed to represent Agency policy nor does mention of trade names or commercial products constitute endorsement or recommendation for use.

References

Baliff, M. D. and Kelly, K. E. Hexavalent chromium in hazardous waste incineration facilities: from stack emissions to health risks, *AWMA Specialty Conference*, Kansas City, MO, April, 1990.

Barin, I., Knacke, O. and Kubaschewski, O. Thermochemical properties of inorganic substances, supplement, Springer-Verlag, New York, NY (1977).

Barin, I. Thermochemical data of pure substances, VCH Verlagsgesellschaft. New York, NY (1989).

Barton, R. G., Clark, W. D. and Seeker, W. R. (1990). Fate of metals in waste combustion systems, *Combust. Sci. and Technol.*, **74**, 327–342.

CAA - Clean Air Act Amendments (1990). Public Law 101 549, 104 Stat. 2399 2712, Nov. 15.

Chase, M. W. Jr. (1986). JANAF thermochemical tables, 3rd ed., parts I&2, American Institute of Physics, New York, NY.

Draft Method 0013-Determination of hexavalent chromium emissions from stationary sources, (1990) in methods manual for compliance with the BIF regulations, EPA/530-SW-91-010 (NTIS PB91-120006), pp. 3–49 thru 3–69, Washington, DC.

Draft Method 29-Methodology for the determination of metals emissions in exhaust gases from hazardous waste incineration and similar combustion processes, (1990) in methods manual for compliance with the BIF regulations, EPA/530-SW-91-010 (NTIS PB91–120006), pp. 3–1 thru 3–48, Washington, DC.

Ebbinghaus, B. B. (1993). Themmodynamics of gas phase chromium species: the chromium chlorides, oxychlorides, fluorides, oxyfluorides, hydroxides, oxyhydroxides, mixed oxyfluorochlorohydroxides, and volatility calculations in waste incineration processes, *Combust. & Flame*, **101**, 119–137.

Ebbinghaus, B. B. (1995). Themmodynamics of gas phase chromium species: the chromium oxides, chromium oxyhydroxides, and volatility calculations in waste incineration processes, *Combust. & Flame*, **93**, 311 338.

Federal Register, **56**, (35) Feb. 21, 1991, U.S. EPA Office of Solid Waste, Guidance on metal and hydrogen chloride controls for hazardous waste incinerators, volume IV of the hazardous waste incineration guidance series, Hazardous waste: boilers and industrial furnaces; burning of hazardous wastes, **7134**, Washington, DC.

Fontijn, A., Blue, A. S., Narayan, A. S. and Bajaj, P. N. (1994). Gas-phase oxidation kinetics of toxic metals at incinerator temperatures. The reactions of chromium atoms with HCl, N_2O, Cl_2, and O_2, *Combust. Sci. and Technol.*, **101**(1–6), 59 73.

Garg, S. (1992). Technical implementation document for EPA's boiler and industrial furnace regulations, EPA-530/R-92–011 (NITS PB92–154947), U.S. EPA, Office of Solid Waste, Washington, DC.

Gordon, S. and McBride, B. J. (1986). Computer program for calculation of complex chemical equilibrium compositions, rocket performance, incident and reflected shocks, and Chapman-Jouguet detonations, NASA SP-273, Interim Revision.